Available online at www.sciencedirect.com
ScienceDirect
Journal of Power Sources 173 (2007) 950–958
JOURNAL OF POWER SOURCES
www.elsevier.com/locate/jpowsour

Analyses of one-step liquid hydrogen production from methane and landfill gas

Cunping Huang *, Ali T-Raissi

University of Central Florida, Florida Solar Energy Center, 1679 Clearlake Road, Cocoa, FL 32922-5703, United States

Received 5 June 2007; received in revised form 2 August 2007; accepted 3 August 2007
Available online 15 August 2007

Abstract

Conventional liquid hydrogen (LH_2) production consists of two basic steps: (1) gaseous hydrogen (GH_2) production via steam methane reformation followed by purification by means of pressure swing adsorption (PSA), and (2) GH_2 liquefaction. LH_2 produced by the conventional processes is not carbon neutral because of the carbon dioxide (CO_2) emission from PSA operation. A novel concept is herein presented and flowsheeted for LH_2 production with zero carbon emission using methane (CH_4) or landfill gas as feedstock. A cryogenic process is used for both H_2 separation/purification and liquefaction. This one-step process can substantially increase the efficiency and reduce costs because no PSA step is required. Furthermore, the integrated process results in no CO_2 emissions and minimal H_2 losses. Of the five flowsheets presented, one that combines low and high temperature CO/CH_4 reforming reactions in a single reactor shows the highest overall efficiency with the first and second law efficiencies of 85% and 56%, respectively. The latter figure assumes 10% overall energy loss and 30% efficiency for the cryogenic process.
© 2007 Elsevier B.V. All rights reserved.

Keywords: Liquid hydrogen; Cryogenic separation; Chemical simulation; Steam methane reforming; Water gas shift reaction

1. Introduction

In addition to being a propellant for space vehicles, liquid hydrogen (LH_2) can be utilized for on-board hydrogen storage in polymer electrolyte membrane fuel cell (PEMFC) powered vehicles. On-site production of LH_2 can facilitate its use in transportation applications. Presently, LH_2 is produced by liquefaction of high purity gaseous hydrogen (GH_2) generated by steam methane reformation (SMR) followed by pressure swing adsorption (PSA) purification, with up to 85% H_2 recovery and at 99.95% purity. One major disadvantage of PSA is that the effluent, containing high concentrations of carbon monoxide (CO), H_2 and methane (CH_4), is burned to recover the energy value of the combustible gases, thereby wasting CH_4 and CO as potential H_2 producing species as well as increasing the emission of greenhouse gases. Besides H_2 recovery efficiency, H_2 purity is another important parameter when used especially in PEMFC and rocket propulsion applications that typically require hydrogen purity at 99.9995% level or higher. For example, very low-levels (∼10 ppmv) of contaminants such as CO and hydrocarbons can deactivate platinum catalysts used in PEMFC membrane electrode assemblies [1]. It is apparent that GH_2 production through PSA purification may not be sufficient for many applications and deep removal of CO and other contaminants is often required. Various techniques including CO preferential oxidation, CO methanation and electrochemical water gas shift reaction have been used to achieve high hydrogen purity [1].

The cryogenic separation and purification process is a well-established technology for recovery and purification of hydrogen in refineries and the petrochemical industry [2]. Conventional cryogenic H_2 purification utilizes partial condensation to separate H_2 from impurities with higher boiling points, such as H_2O, CO, CO_2, CH_4, and hydrocarbons. Because of the high relative volatility of H_2 as compared to these impurities, cryogenic processes can separate H_2 from off-gases with a very high recovery efficiency at purity levels that far exceed those obtained from PSA or membrane separation processes [3,4].

It should be noted that the efficiency of a cryogenic system is a strong function of heat recovery. The optimization of the heat exchanger system is essential in improving its first and second law efficiencies. Before chemical engineering simulation became widely available, process design and efficiency

* Corresponding author. Tel.: +1 321 638 1505; fax: +1 321 638 1010.
E-mail address: chuang@fsec.ucf.edu (C. Huang).

0378-7753/$ – see front matter © 2007 Elsevier B.V. All rights reserved.
doi:10.1016/j.jpowsour.2007.08.018

Nomenclature

CE	cooling energy
CompE	compressor energy requirement
CondE	condenser energy requirement for the distillation column
HE	heating energy
HX	heat exchanger
n_{LCO_2}	number of moles of liquid carbon dioxide
n_{LH_2}	number of moles of liquid hydrogen
R_{CO_2/LH_2}	amount of carbon dioxide (g) produced per gram of liquid hydrogen collected
R_{Energy/LH_2}	input energy per mole of liquid hydrogen collected
ReE	reboiler energy requirement for the distillation column

Greek letters

η_{Carnot}	Carnot efficiency
$\eta_{Separation}$	cryogenic hydrogen separation efficiency
η_{1st}	first law efficiency
η_{2nd}	second law efficiency

determination were very difficult and time consuming. For this reason, the development and widespread application of cryogenic separation processes have been limited. If cryogenic purification and H_2 liquefaction could be combined into a single process, the capital cost of the cryogenic separation would be a small portion on the LH_2 production cost. The objective of this paper is to demonstrate the viability of using CH_4 and landfill gas (LFG) as feedstocks for producing hydrogen. Five scenarios have been flowsheeted and analyzed in this paper utilizing Aspen Technologies chemical process simulation (CPS) platforms.

2. LH_2 production and the efficiency of cryogenic separation

Fig. 1 depicts a schematic diagram of the LH_2 production process. Hydrogen rich gaseous mixture is produced via methane autothermal reformation followed by cryogenic separation. In the cryogenic process, water vapor is separated in the first stage of the process and liquid CO_2 removed from the gas stream in the second stage. Finally, in the third stage, H_2 is separated from the gaseous mixture containing CO and CH_4. The mixture is then fed into the steam methane reformer to produce additional hydrogen that is then mixed with the primary stream from the authothermal reactor and sent to the cryogenic separation unit. Low temperature and high purity H_2 extracted from the CO and CH_4 mixture is then cooled to form LH_2, without any H_2 losses. Since there is no outlet for either CO or CH_4, theoretically, the recovery of CO and CH_4 should be 100%. CO_2 collected in the cryogenic process has high purity making it useful in a variety of applications. Because thermal heat and cooling energy can be recovered using heat exchangers, this process can be more efficient than the conventional LH_2 plants. The overall process can be summarized as follows:

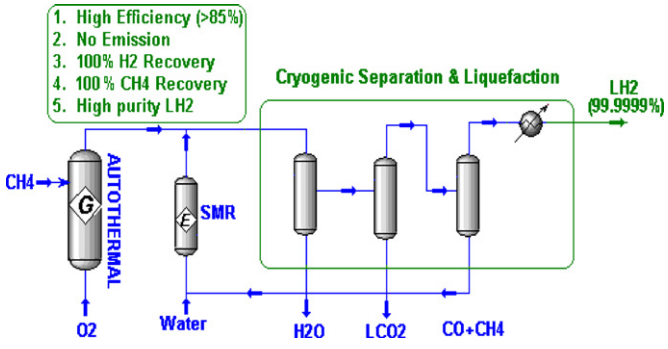

Fig. 1. Schematic diagram of innovative liquid H_2 production process.

methane(from natural gas or LFG) + water + O_2

→ gasmixture → cryogenic separation & liquefaction

→ LH_2

As discussed above, a cryogenic separation process can be cost effective and efficient if H_2 separation and liquefaction are combined into a single process. But, this makes thermodynamic calculation of cryogenic separation efficiency more complicated. The energy required for cryogenic separation of H_2 from a gas mixture consists of two parts: H_2 separation energy and H_2 liquefaction energy. The cooling energy input for separating components of a gas mixture can be recovered to a large extent by using heat exchangers. Therefore, the total energy needed for LH_2 production, by the cryogenic process of Fig. 2, using hydrogen rich gas mixture containing CO, CH_4, CO_2, and H_2O is:

$$\Delta H_{Total} = (\Delta H_{Cooling} + \Delta G_{Separating} + \Delta H_{Recovering})_{Gas\ mixture} + (\Delta H_{Liquefaction})_{Hydrogen} \quad (1)$$

where $\Delta G_{Separating}$ is the Gibbs free energy change for separating a component in the mixture. During the cryogenic separation, H_2 is cooled progressively until liquefied. Therefore, the cryogenic separation efficiency (First Law efficiency) for LH_2 production is:

$$\eta_{Separation} = \frac{(\Delta H_{Cooling} + \Delta H_{Liquefaction})_{Hydrogen}}{\Delta H_{Total}} \quad (2)$$

In principle, the separation efficiency can be determined from thermodynamics. However, due to the complexities involved in determining heat recoveries in the heat exchangers, its evaluation is somewhat difficult. Furthermore, separation temperatures are different from one component to another and vary with system pressure. Calculation of the cooling energy and heat recovery is also complicated. Additionally, in a cryogenic process, at elevated pressures, a gas mixture cannot be considered an ideal gas, thus, leading to further complications. Accordingly, the precise determination of separation efficiency would be difficult using conventional thermodynamic methods.

For this work, we have used Aspen Technologies' CPS platforms. Fig. 2 illustrates a HYSYS flowsheet for separating and liquefying H_2 from a hydrogen rich gas mixture. We note that

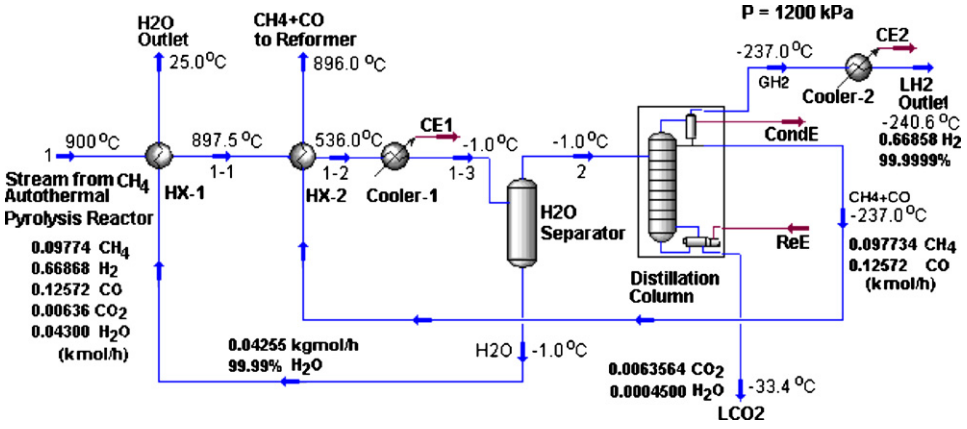

Fig. 2. Separation efficiency calculation ($P = 1.2$ MPa, $\Delta H_{Total} = 2.666 \times 10^4$ kJ h^{-1}, hydrogen recovery exceeds 99.99%).

at cryogenic state and elevated pressures, both vapor and liquid phases are far from being ideal. In our simulation, the Peng Robinson Equation of State was selected as the fluid package since it is considered applicable to both non-ideal vapors and solutions. The tray efficiencies of the distillation column (Fig. 2) are assumed to be 95%. Idealized heat exchangers were assumed with no heat loss. Stream 1 is a feed stream containing H_2 rich gas mixture from an autothermal CH_4 pyrolysis reactor containing H_2, CO, CO_2, CH_4, and H_2O. The composition of the mixture is calculated from a Gibbs reactor using AspenPlus^{TM} CPS. The inlet stream to the Gibbs reactor contains 0.452 kmol of CH_4 and 0.0904 kmol of O_2, respectively, at a temperature of 900 °C and 1200 kPa. In order to calculate the total energy requirement (ΔH_{Total}, Eq. (2)) for cooling and liquefaction of pure H_2, a simple flow diagram (Fig. 3) was used—subject to conditions identical to those in Fig. 2. Based on Figs. 2 and 3, the energy input to both pure H_2 liquefaction (0.66858 kmol h^{-1}) and gas mixture can be determined.

In the case of 71.02% of GH_2 concentration in the gas mixture, the separation efficiency defined by Eq. (2) is $\eta_{Separation}\% = (2.281 \times 10^4 / 2.666 \times 10^4) \times 100\% = 85.56\%$. In other words, 86.56% of the energy is used for LH_2 production, while 13.44% is consumed for cryogenic separation of H_2O, CO_2, CO, and CH_4. It should be noted that several factors contribute to the separation efficiency. For example, concentration of H_2 plays an important role in the efficiency calculations. Eq. (2) predicts that for two extreme conditions (*i.e.* the inlet H_2 concentrations of 100% and 0% to the cryogenic separation and liquefaction system shown in Fig. 2) efficiencies are 100% and 0%, respectively. Fig. 4 depicts the cryogenic separation efficiency as a function of inlet GH_2 concentration. The efficiency

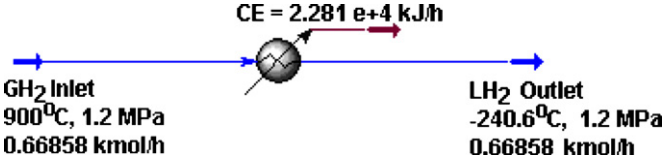

Fig. 3. H_2 cooling and liquefaction energy calculation ($P = 1.2$ MPa, $\Delta H_{CE\text{-}2} = 2.281 \times 10^4$ kJ h^{-1}).

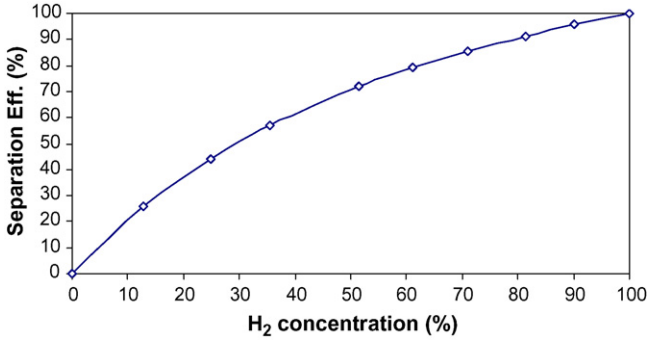

Fig. 4. Separation efficiency vs. inlet GH_2 concentration.

increases nonlinearly with increasing GH_2 concentration. If a separation efficiency of 70% is required, concentration of inlet GH_2 must be higher than 50 mol% in the gaseous mixture. On the other hand, if the H_2 recovery rate is defined as (LH_2 outlet flow rate)/(GH_2 flow rate) × 100%, Figs. 2 and 3 show that the recovery rate in a cryogenic separation system increases with increasing inlet GH_2 concentration. The extent of H_2 in the outlet CO and CH_4 streams is affected by the separation efficiency of the distillation column. The components CO, CH_4, and H_2O do not significantly influence the separation efficiency since the cooling energy required for separating these species can be recovered in the heat exchangers. The outlet CO_2 in liquid form (LCO_2) makes it easier to transport, store and/or sequester. Note that required LH_2 purity does not have a strong effect on the separation efficiency because the relative volatility of H_2 to CH_4 in a typical cryogenic process is greater than 200 [2].

3. Processes for LH_2 production from methane and landfill gas

There are several conventional technologies for production of H_2 from CH_4, including steam reforming (SMR), partial oxidation, pyrolysis, autothermal pyrolysis, and autothermal SMR. Carbon monoxide (CO), the intermediate generated from these processes (except in the case of pure CH_4 pyrolysis that produces

only solid carbon and H_2), can undergo high and low temperature water gas shift reactions (WGSR) to produce more H_2 and CO_2. Therefore, by combining these processes with a cryogenic separation process, a number of flow diagrams for production of LH_2 directly from CH_4 can be conceived. In order to reduce the production of CO_2, we selected CH_4 autothermal pyrolysis for GH_2 production. The energy required for CH_4 pyrolysis is derived from partial combustion of CH_4, in which enough heat is generated to allow decomposition of any remaining CH_4, resulting in a thermo-neutral process. The outlet stream from the autothermal reactor consists of CH_4, H_2, CO, CO_2, and H_2O. The gaseous mixture is separated cryogenically into individual components. In some case studies no CO and CH_4 separation were needed, and the mixture was combined with H_2O and recycled to a high temperature gas conditioning reactor (HTGCR) or a low temperature gas conditioning reactor (LTGCR) to generate more H_2. The product stream from either HTGCR or LTGCR was mixed with the main stream from the CH_4 autothermal pyrolysis reactor and sent to the separation unit. Based on the processes discussed above, five flowsheets were constructed for LH_2 production as follows:

- *Flowsheet I*. CH_4 and CO are not separated; the gaseous mixture enters HTGCR and LTGCR.
- *Flowsheet II*. CH_4 and CO are not separated; both gas mixtures enter HTGCR.
- *Flowsheet III*. CH_4 and CO are separated; CH_4 enters SMR and CO enters WGSR.
- *Flowsheet IV*. CH_4 and CO are separated; CH_4 is sent back to autothermal pyrolysis while CO is fed to WGSR.
- *Flowsheet V*. LH_2 is produced from landfill gas; a mixture of CH_4 and CO enters HTGCR.

Flowsheet I is shown in Fig. 5 and the process can be separated into three sections:

(I) *CH_4 autothermal decomposition*. CH_4 and O_2 gases are heated to 900 °C and mixed in a Gibbs reactor operating isothermally. Because the objective of this simulation was to calculate the energy requirement, CH_4 decomposition during the heating process was assumed not to occur but take place in the isothermal Gibbs reactor. The ratio of CH_4 to O_2 (CH_4:O_2 = 5:1) indicates that 20% of the CH_4 is oxidized to produce the heat required for the pyrolysis of the remaining CH_4 [2]. After separating solid carbon, the gas mixture containing CH_4, H_2, CO, CO_2, and H_2O was then sent to cryogenic separation.

(II) *Cryogenic separation*. Here, H_2O and pure CO_2 are separated as liquids while the remaining gas mixture is distilled to separate the high purity GH_2 from CH_4 and CO. Low temperature GH_2 is then liquefied to LH_2. A gaseous stream containing CH_4 and CO is not separated and is recycled to the recirculation loop.

(III) *HTGCR and LTGCR recirculation loop*. H_2 is produced from the remaining CH_4 and CO in HTGCR and LTGCR, based on the HYSYS 3.0.1 equilibrium reactions:

$$CO + H_2O \rightarrow H_2 + CO_2$$

$$CH_4 + H_2O \rightarrow 3H_2 + CO$$

The outlet stream (R6) is mixed with the main stream 1–0 from section (I) and sent to section (II) for the component separation.

The thermal heat energy generated in the process is recovered via many ideal heat exchangers having heat recovery efficiency equal to 100%. The details of the heat exchanger arrangement are shown in Fig. 5. Likewise, Figs. 6–9 depict Flowsheets II–V. Note that Flowsheet V was developed for the production

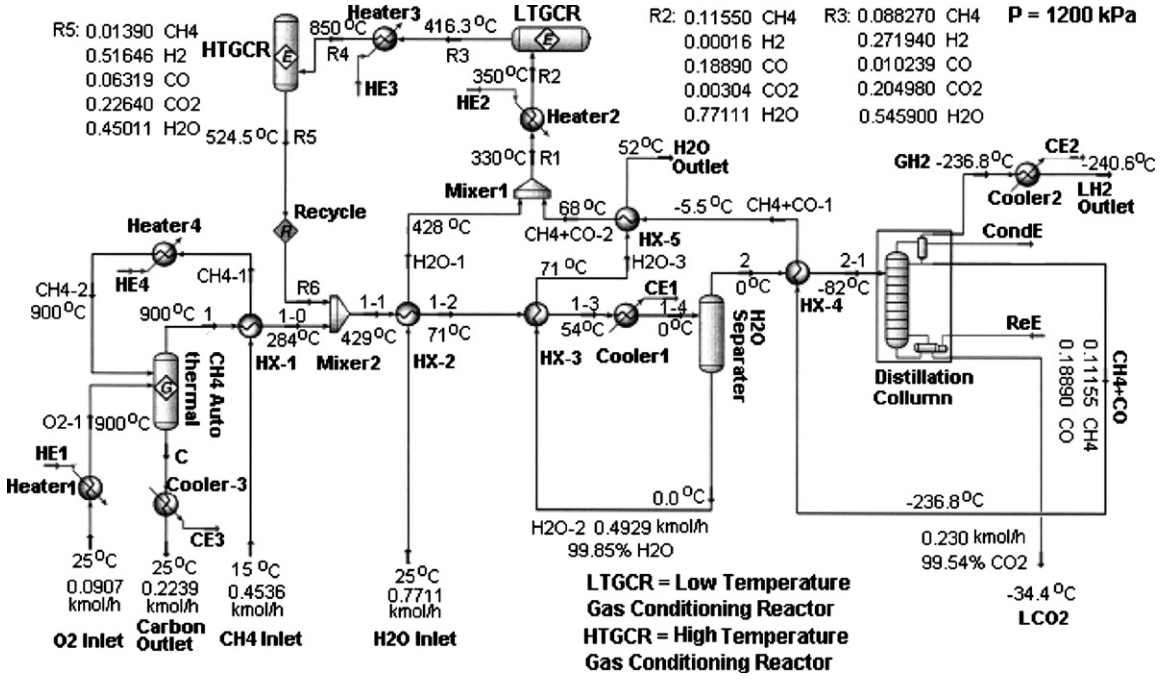

Fig. 5. Flowsheet I (no CH_4 and CO separation, the gaseous mixture undergo LTGCR and HTGCR).

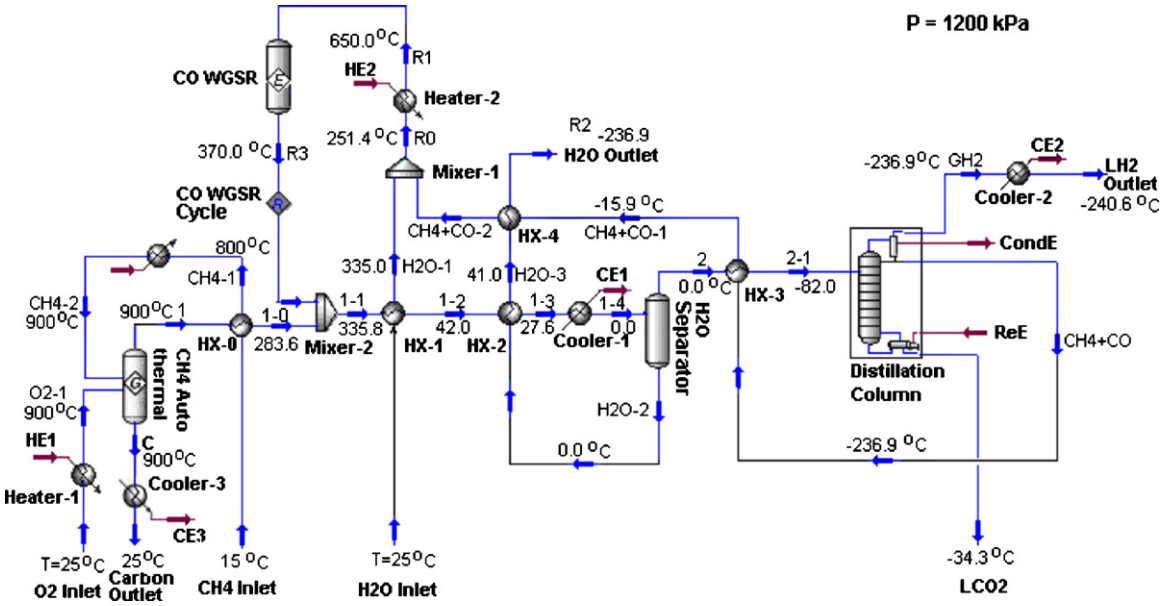

Fig. 6. Flowsheet II (no methane and carbon monoxide separation, no SMR).

of LH_2 from landfill gas (LFG), in which LFG is purified by a cryogenic process to produce pure CH_4 and N_2. CH_4 is then fed into an autothermal reformer to generate solid carbon and a hydrogen rich gas mixture. Before the cryogenic purification process, hydrogen sulfide (H_2S) must be removed from LFG to avoid the deactivation of catalysts. Oxygen is also removed from LFG prior to the cryogenic separation process. Because LFG is saturated with water vapor at room temperature and 1 atm, H_2O concentration can be calculated using HYSYS program as depicted in the landfill gas inlet stream. Although cryogenic LFG purification is a capital intensive process, the combination of purification and LH_2 production may result in some benefits. Firstly, CH_4 recovery can reach 99.99% with purity levels as high as 99.93%. Even though a higher purity can be achieved by adjusting the cooling temperature in the N_2 separator, obtaining higher CH_4 purity requires considerable energy input. For example, when methane purity is 99.93% and nitrogen purity is 99.96%, CondE-3 and ReE-3 are, respectively, 5246 kJ h^{-1} and 2244 kJ h^{-1}. If the purity levels are increased to 99.99% for CH_4 and 99.996% for N_2, CondE-3 and ReE-3 energy requirements increase to 70,410 kJ h^{-1} and 67,410 kJ h^{-1}, respectively. Secondly, in a cryogenic process, individual components can be extracted as valuable co-products in the process, *e.g.* high purity liquid N_2 and CO_2. It must be

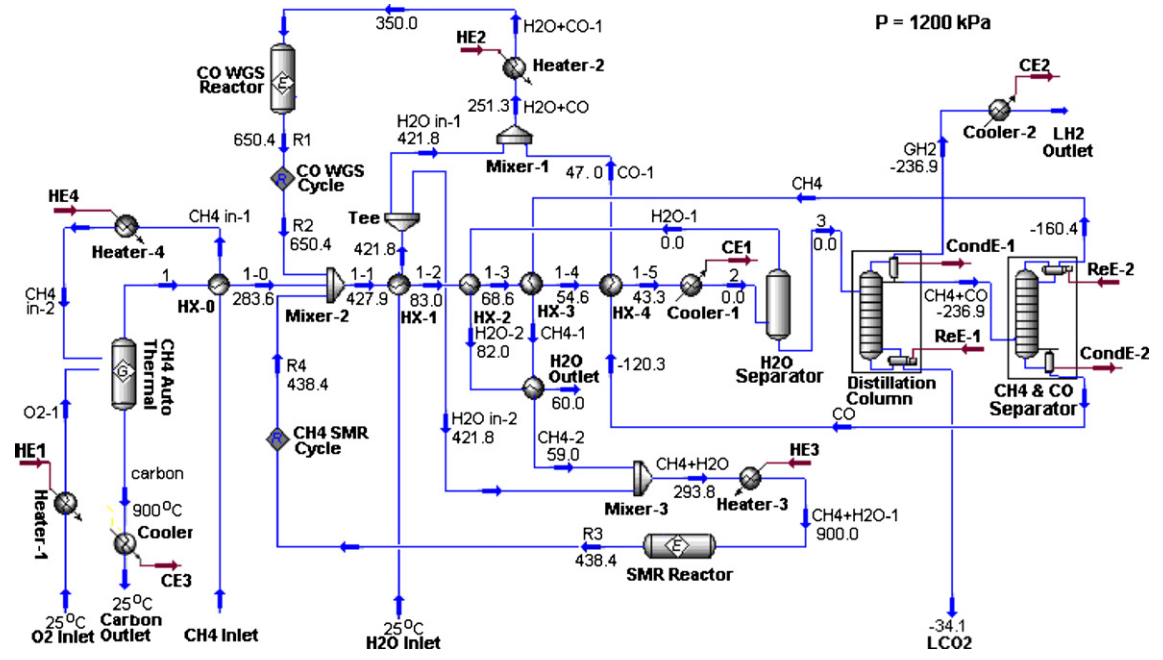

Fig. 7. Flowsheet III (CO and CH_4 are separated; CO undergoes WGSR while CH_4 SMR).

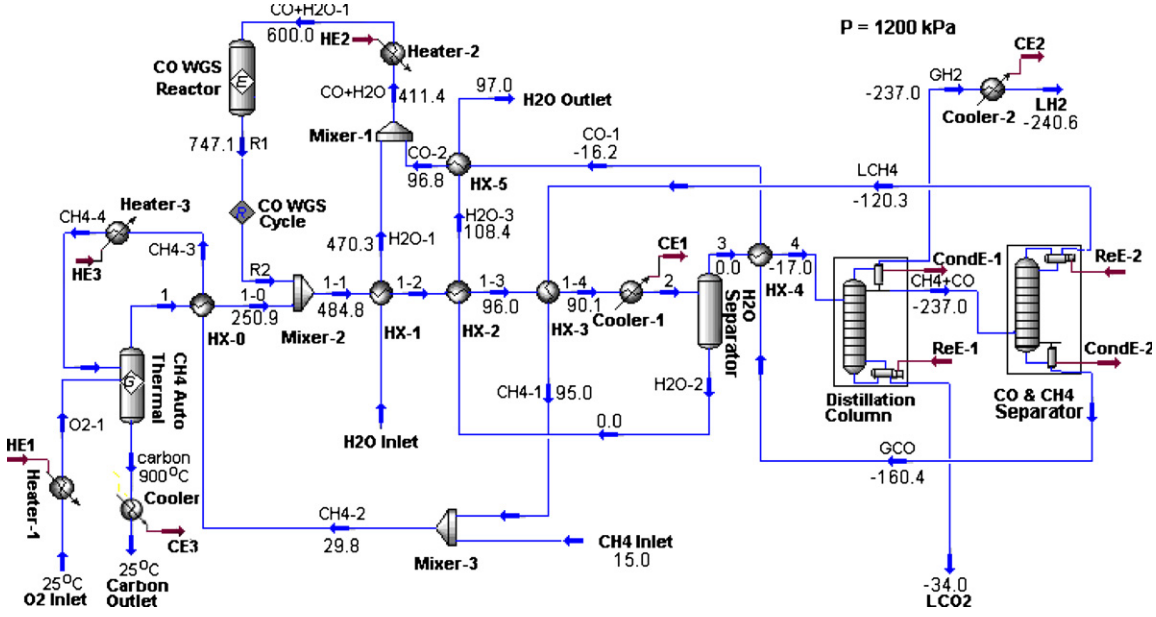

Fig. 8. Flowsheet IV (CO and CH_4 are separated; CO undergoes WGSR while CH_4 pyrolysis).

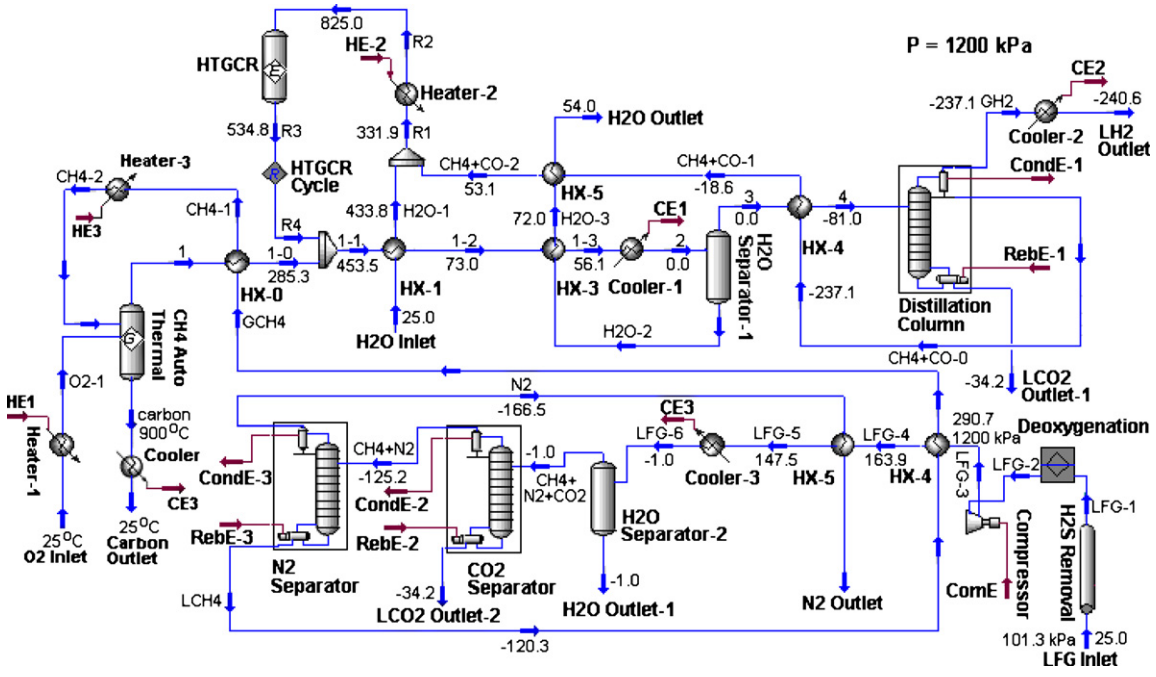

Fig. 9. Flowsheet V. LH_2 production through landfill gas (no CH_4 and CO separation, the gaseous mixture undergo a HTGCR).

pointed out that a practical application of the cryogenic process depends upon both the efficiency and cost of the process.

4. Results and discussion

4.1. The first and second law efficiencies

The first law and second law efficiencies are defined as:

$$\eta_{1st} = \frac{n_{Hydrogen}(\Delta H_{Combustion} + \Delta H_{LH_2})_{Hydrogen}}{(n_{Methane}\,\Delta H_{Combustion})_{Methane} + \Delta H_{Total}} \times 100\% \quad (3)$$

$$\eta_{2nd} = \frac{n_{Hydrogen}(\Delta G_f^\circ + \Delta H_{LH_2}\eta_{Carnot})}{(n_{Methane}\,\Delta H_{Combustion})_{Methane} + \Delta H_{Heating} + \Delta H_C/\eta_C} \times 90\% \quad (4)$$

where CH_4 combustion $\Delta H_{Combustion} = \Delta H^\circ_{298\,K} = 802.6\,kJ\,mol^{-1}$. Hydrogen high heating value $\Delta H_{Combustion} = \Delta H^\circ_{f298\,K} = 285.9\,kJ\,mol^{-1}$. $n_{Methane}$ and $n_{Hydrogen}$ refer to number of moles of input CH_4 and H_2 generated, respectively; $\Delta G_f^\circ = 228.5\,kJ\,mol^{-1}$ is the Gibbs free energy change for the formation of 1 mol of water. While H_2 cooling and liquefaction energy $(\Delta H_{Cooling} + \Delta H_{Liquefaction})_{Hydrogen}$, calculated from

Table 1
Energy balance and efficiencies of the five scenarios

Energy streams	Scenario I	Scenario II	Scenario III	Scenario IV	Scenario V
HE1 (kJ h^{-1})	2624.0	2624.0	2624.0	3193.0	2624.0
HE2 (kJ h^{-1})	820.0	17,450.0	1574.0	5584.0	21,710.0
HE3 (kJ h^{-1})	20,560.0		23,030.0		
HE4 (kJ h^{-1})	3452.0	3452.0	3452.0	4200.0	3453.0
CE1 (kJ h^{-1})	5840.0	2725.0	4813.0	11,100.0	2973.0
CE2 (kJ h^{-1})	563.6	570.7	568.4	449.8	558.2
CE3 (kJ h^{-1})	−3420.0	−3420.0	−3420.0	−4922.0	−3420.0
CE4 (kJ h^{-1})					6705.0
CondE (kJ h^{-1})	12,910.0	13,010.0	20,880.0	12,350.0	13,060.0
ReE (kJ h^{-1})	911.5	916.3	1173.0	456.3	934.3
CondE-2 (kJ h^{-1})			5369.0	2768.0	9764.0
ReE-2 (kJ h^{-1})			1576.0	768.4	1836.0
CondE-3 (kJ h^{-1})					5246.0
ReE-3 (kJ h^{-1})					2244.0
CompE (kJ h^{-1})					11,010
Total (kJ h^{-1})	44,261.1	37,328.0	61,639.4	35,947.5	78,697.5
LH_2 (kmol h^{-1})	1.1852	1.1852	1.1852	0.9506	1.1852
LCO_2 (kmol h^{-1})	0.2286	0.2286	0.2285	0.1318	0.2290
First law efficiency (%)	85.34	86.81	81.85	87.11	78.70
Second law efficiency (%)	55.21	56.95	52.09	44.83	50.89
ΔH (kJ kmol^{-1} LH_2)	37,345	31,495	52,008	37,816	66,400
Ratio (CO_2/H_2) (g g^{-1})	4.211	4.211	4.209	3.027	4.219

Fig. 2, is equal to $n_{\text{Hydrgoen}} \times 34{,}120\,\text{kJ h}^{-1}$. Since LH_2 can serve as a low-temperature heat sink for a heat engine operating between room temperature and −240.6 °C, the heat flow from the hot source (GH_2 at 25 °C) to the cold sink (LH_2 at −240.6 °C) is: $\Delta H_{LH_2} = 8147.68\,\text{kJ mol}^{-1}$, with Carnot efficiency of $\eta_{\text{Carnot}} = (298.15 - 32.55)/298.15 \times 100\% = 89.08\%$.

The work produced from the engine can be calculated as follows: $\Delta H_{\text{LH2}} \times \eta_{\text{Carnot}}$. Considering heat losses and leakage in the cryogenic system, we assume cryogenic process efficiency, η_C, of 30% (input electrical energy to cooling energy required for separation and liquefaction of hydrogen). In addition to the energy required for the entire process, one must consider the heat leakage and heat recovery losses throughout the process. Assume that 10% of total heat is lost in the process; the second law efficiency is assumed to be less than that calculated from Eq. (4) to compensate for the ideal heat exchanger assumption.

To further evaluate an LH_2 production process, two parameters were used that are defined as: R_{Energy/LH_2}, that is the total energy consumption per mole of LH_2 produced, and R_{CO_2/LH_2}, that refers to the weight (g) of CO_2 produced per gram of LH_2 generated. These parameters can be used for a general comparison with the conventional processes described in the literature. It should be noted that, since liquid carbon dioxide (LCO_2) is produced during cryogenic separation, instead of directly releasing this greenhouse gas into the atmosphere, LCO_2 can be used as a co-product or solidified and sequestered to reduce its environmental impact.

$$R_{\text{Energy}/LH_2} = \frac{\Delta H_{\text{Total}}}{n_{LH_2}} \tag{5}$$

$$R_{CO_2/LH_2} = \frac{n_{CO_2} \times 44}{n_{LH_2} \times 2} \tag{6}$$

Table 1 lists the energy balance and efficiencies for the five flowsheets discussed above. The first law efficiencies, after taking cooling effect of LH_2 into account, for four of the five scenarios are calculated to be over 81% (except Flowsheet V that is 78.7%). Even with added energy input for separating CO and CH_4, Scenario IV achieves the highest first law efficiency (87.11%). The first law efficiency for Flowsheet III is calculated to be 81.85%. Since Flowsheet IV does not include an SMR as in Flowsheet III, simulation results indicate that inclusion of an SMR process results in consumption of a large portion of the input energy, while the use of a CH_4 autothermal reformer reduces the total input energy requirement.

A comparison of the Flowsheets I and II reveals that combining HTGCR and LTGCR into one unit would reduce the energy input required, thereby increasing first law efficiency of the process. Although the total energy input for Flowsheet IV is the lowest amongst all the five flowsheets considered (*i.e.*

Table 2
Total mass balance for Scenario II

Inlet components (kmol h^{-1})	
CH_4	0.4536
O_2	0.0907
H_2O	0.7711
Outlet components (kmol h^{-1})	
LH_2	1.1852
LCO_2	0.2290
Carbon	0.2239
H_2O	0.4922

Table 3
SMR temperature effects on the stability of Scenario II

Temperature (°C)	HE2 (kJ h^{-1})	CE1 (kJ h^{-1})	CE2 (kJ h^{-1})	CondE (kJ h^{-1})	ReE (kJ h^{-1})	ΔH_{Total} (kJ h^{-1})	1–1 flow (kmol h^{-1})	LH_2 (kmol h^{-1})	LCO_2 (kmol h^{-1})	R_{Energy/LH_2} (kJ kmol^{-1})	R_{CO_2/LH_2} (g g^{-1})
500	21740	−5937	629	24300	788	44176	2.673	1.185	0.2290	37279	4.25
550	19800	−3807	605	20580	766	40599	2.452	1.185	0.2288	34261	4.25
600	18500	−2293	588	18110	747	38308	2.305	1.185	0.2287	32327	4.25
650	17750	−1271	577	16530	732	36974	2.212	1.185	0.2286	31202	4.24
700	17960	−426	570	15820	725	37304	2.170	1.185	0.2285	31481	4.24
750	19190	396	567	15840	724	39373	2.173	1.185	0.2285	33226	4.24
800	20790	1322	564	16100	727	42159	2.192	1.185	0.2285	35577	4.24
850	22730	2470	562	16460	730	45607	2.180	1.185	0.2286	38487	4.24
900	24750	3689	558	16920	733	49306	2.225	1.185	0.2286	41609	4.24

35,947.5 kJ h^{-1}), its second law efficiency is calculated to be the lowest (44.83%) as well. The reason for this is that the amount of LH_2 produced (0.9506 mol) is less than that generated (1.1852 mol) in the other four flowsheets. The second law efficiencies of Flowsheets I and II are similar. Flowsheet II combines HTGCR and LTGCR into one so it is expected that the capital cost for the process will be lower. Results of Table 1 also show that the cooling energy share of the total energy input is a major contributor to the second law efficiency calculations since the cooling process is a generally low efficiency process (about 35%). Increasing CH_4 and CO conversions during HTGCR/LTGCR or SMR/WGSR increases the second law efficiencies of these processes.

4.2. Total material balance and methane conversion

Let us consider Flowsheet II as an example to demonstrate the manner in which the calculation of material balances was carried out. Table 2 shows the total flow rates for components input and output. The material balance calculations were performed as follows.

- Carbon balance = 0.4536 − 0.2290 − 0.2239 = 0.0007 kmol h^{-1}.
- Hydrogen balance = 2 × 0.4536+(0.7711 − 0.4922) − 1.1852 = 0.00094 kmol h^{-1}.
- Oxygen balance = 0.0907 + (0.7711 − 0.4922)/2 − 0.2290 = 0.0012 kmol h^{-1}.
- Hydrogen produced from methane = 2 × 0.4536 = 0.9072 kmol h^{-1}.
- Hydrogen produced from water = 0.711 − 0.4922 = 0.2789 kmol h^{-1}.
- Percentage of hydrogen from methane = 0.9072/1.1852 × 100% = 76.5%.
- Percentage of hydrogen from water = 0.2789/1.1852 × 100% = 23.5%.

These results indicate satisfactory material balances for all input and output elements. Results also show that more than 75% of total hydrogen is produced from methane while less than 25% comes from water splitting. With an increase of H_2 production through CH_4 pyrolysis, the CO_2 to H_2 ratio will be reduced to 4.21 in comparison to SMR ($CH_4 + 2H_2O = 4H_2 + CO_2$) from which 50% of H_2 is produced from CH_4 and 50% comes from water. The CO_2 to H_2 ratio is 1*44/(4*2) = 5.5. Since there is no CO or CH_4 discharged during the process, both CH_4 conversion and H_2 yield would be 100%. These results further illustrate the benefits of using a cryogenic process for LH_2 production.

4.3. Process stability considerations

The stability of a process is a measure of the capability of the process to maintain steady state when operating conditions change. Because CH_4 and CO remain within the cryogenic process and are recycled, the entire process remains in a steady state operating condition when, for example, the catalyst is gradually deactivated or some disturbance occurs within the system. One way to simulate catalyst deactivation in SMR or WGSR is to vary the reaction temperature in order to affect the reaction rate. CO and CH_4 conversion will vary with the reaction temperature. The variation of the conversions within SMR or WGSR will, in turn, affect the steady state of the process. Table 3 depicts that even with a relatively wide variation of the SMR temperature range (from 500 °C to 900 °C), the output LH_2 and LCO_2 remain unchanged. The ratio of total energy per mole of LH_2 produced and the system efficiencies vary slightly. Thus, the cryogenic process described here offers a more efficient alternative to LH_2 production than the present conventional processes.

5. Conclusions

Five processes combining separation and production of liquid hydrogen, directly from methane and landfill gas, were described and flowsheeted. The chemical process simulation results for the first and second law efficiencies, the extent of greenhouse gas emissions and process stability considerations show that highly efficient processes for production of high purity LH_2 are possible by integrating H_2 production and liquefaction processes. For an optimized flowsheet, the extent of H_2 recovery can be 99.99% with purity levels as high as 99.9999% and methane conversion efficiencies of up to 99.99%. As a by-product of liquid H_2 production, high purity liquid CO_2 is also generated as a value added co-product. The total thermal efficiencies of the processes considered exceed 81% and 79% for methane and landfill gas, respectively. The highest energy efficiency calculated is 57% for methane and 51% for landfill gas under the assumption of 10%

heat loss and 30% efficiency for the cryogenic process used. The ratio of CO_2 to H_2 mass in these processes falls between 3.027 g g^{-1} and 4.219 g g^{-1}. If the input electrical energy to the system is generated from a renewable resource, such as solar or wind, conversion of CH_4 to liquid H_2 via processes considered would be essentially zero emission.

Acknowledgment

We acknowledge the support of this work by NASA-GRC under Grant No. NAG3-2751 which is greatly appreciated.

References

[1] C. Huang, R. Jiang, M. Elbaccouch, N.Z. Muradov, J.M. Fenton, J. Power Sources 162 (2007) 563–571.
[2] H.C. Rowles, D.M. Nicholas, H.L. Vines, M.F. Hilton, Energy Prog. 6 (1) (1986) 25–32.
[3] N.Z. Muradov, C. Huang, A. T-Raissi, Proceedings of the 15th World Hydrogen Energy Conference, Yokohama, Japan, June 27–July 2, 2004.
[4] N.Z. Muradov, F. Smith, C. Huang, A. T-Raissi, Catal. Today 116 (2006) 281–288.